Desalination and Water Treatment
www.deswater.com
doi: 10.5004/dwt.2018.22067

106 (2018) 251–266
February

An insight into properties and mechanisms of a dithiocarbamate chelating agent for the removal of toxic metal ions from metallic mine wastewater

Fei Feng[a], Daishe Wu[a], Jinbao Wan[a], Hongwei Sun[b], Rong Wang[a,]*

[a]*School of Resources, Environmental & Chemical Engineering, Nanchang University, Nanchang 330031, P. R. China; Key Laboratory of Poyang Lake Environment and Resource Utilization, Ministry of Education, Nanchang 330047, China,*
Tel. 86-791-83969985, Fax 86-791-83969583, email: wangrong@ncu.edu.com (R. Wang)
[b]*Department of Chemistry, Nankai University, Tianjin 300071, China*

Received 9 December 2017; Accepted 14 February 2018

ABSTRACT

The experimental results proved that a liquid and commercial chelating agent (DTCR) with dithiocarbamate (DTC) groups could be used to further remove toxic metal ions from the simulated metallic mine wastewater with trace amount of mixed metal ions. Under the optimized operating conditions, just a little dosage of DTCR (the volume ratio of DTCR to wastewater about 1:10^4) could make the removal rate of Cr^{3+}, Cu^{2+}, Pb^{2+}, Zn^{2+} and Cd^{2+} in the treated water reach 99.70%, 99.28%, 99.10%, 92.33% and 91.49%, respectively. The residual content of the five ions were 0.003, 0.036, 0.009, 0.383 and 0.085 mg/L, which were all obviously lower than the contents required in the emission standard except of Zn^{2+} and Cd^{2+}. The removal ability followed the order of Cr^{3+}> Cu^{2+}> Pb^{2+}> Zn^{2+}> Cd^{2+}. The characterization revealed that the major functional groups in DTCR were DTC groups (-NCS_2) and amino groups (-NH-, -NH_2 or -NR_2) which were not on DTC groups. The removal mechanisms of these functional groups were investigated by the combination of experimental methods and density functional theory (DFT) calculation, which demonstrated that all the five metal ions could be captured by the metal-ligand bonds between ions and C=S/C-S on DTC groups. But Cr^{3+}, Cu^{2+} and Pb^{2+} could be further captured by the electron donation of N atom on -NH_2 and -NH- which were not on DTC groups. Moreover, Cr^{3+} could be further adsorbed by the secondary N atom on DTC group. The relation between the functional groups and metal ions could be calculated quantitatively based on the removal mechanisms. It could well explain the removal ability of DTCR for different metal ions and provide a scientific guideline for the further modification of chelating agent with DTC groups to improve its removal efficiency for Zn^{2+} and Cd^{2+} in the depth treatment of wastewater with trace amount of mixed toxic metal ions.

Keywords: Toxic metal ions; Dithiocarbamate; Chelating agent; Removal mechanism; Density functional theory

1. Introduction

Poyang Lake regarded as the largest freshwater lake in China, has a significant value of ecology and economy [1]. However, there are many metallic mines in its valley, such as copper mine in Dexing, lead-zinc ore in Qianshan, nonferrous metal ore in Raohe basin and so on. Although most of these mine effluents are in line with the national emission standard defined at the 1990's [2], there are still some toxic metal ions in effluents, since the standard can not keep up with the present demand of environmental protection. The spare and toxic metal ions will be enriched to degrade the water quality of Poyang Lake. Therefore, a deep treatment is urgently required to further reduce toxic metal ions amount in effluents before discharging.

Various methods such as membrane separation [3], ion exchange [4–6], chemical precipitation [7] and adsorption [8–11] have been employed to remove toxic metal ions from

---

*Corresponding author.

1944-3994 / 1944-3986

industrial effluents. But adsorption technique was recognized as one of the most effective method for removing toxic metal ions among these technologies due to the significant advantages including high removal efficiency, simplicity and low cost. Moreover, chelating agents as a kind of adsorption techniques have been developed, which can remove metal contaminants from trace amount cases by strong chelating ability and excellent suitability for large-scale wastewater treatment [12–14].

The present chelating agents can be classified into small molecule and polymers. The former mainly includes amino-carboxyl and dithiocarbamates (DTC) groups [15,16], and the latter can be divided into water-soluble and water-insoluble chelating resins [17,18]. The researches proved that both of water-soluble and water-insoluble chelating resins containing DTC groups had strong binding capacity for many toxic metal ions in the treatment of electroplating effluent or smelting wastewater [19–21]. Considered as a low-cost and environmentally-friendly technique, it will have the potential to overcome the limitations of other removal strategies. However, there are rare reports about the performance of chelating agents in the treatment of metallic mine wastewater with trace amount of mixed metal ions. Most of studies on removal mechanisms are carried out by experiment characterizations [12–21], while the theoretical calculation is rarely used. Using the method of density functional theory (DFT) calculation will provide an insight into the removal nature of a chelating agent for various metal ions, since it allows the possibility of modeling the meal complexes and can provide the information about the structure and energy [22,23]. So the theoretical calculation can overcome the problems connected with experimental tools and be considered as an important supplement to the experimental investigation.

Therefore, the objectives of this paper were: 1) DTCR as a kind of water-soluble chelating resin with DTC groups and a commercial chelating agent with low price, was selected to evaluate its removal performance for mixed toxic metal ions in simulated mine wastewater under a variety of operating conditions; 2) to clarify the major functional structures of DTCR as well as its removal mechanism for different metal ions by the combination of experimental method and theoretical calculation. The results will be beneficial to the further improvement and application of the chelating agent with DTC groups in the depth treatment of metallic mine wastewater in Poyang Lake valley.

2. Material and methods

2.1. Materials, reagents and solutions

The chelating agent investigated in the experiment is DTCR, which is a kind of polymer and water-soluble chelating resin with low price and purchased from Futianbao Environmental Protection Technology Co., Ltd, Shanxi Province, PR China. This agent can be dissolved completely in the aqueous solution over a wide range of pH 4–10, and its molecular mass and density was 341.3 g·mol^{-1} and 1.23 g·cm^{-3} (25°C), respectively. If the initial concentration of metal ions was quite low in the waste water, the agent would be best to be diluted by deionized water before the usage.

The published reference [1] and the content analysis in our original experiments demonstrated that there are five kinds of toxic metal ions (Cu^{2+}, Zn^{2+}, Pb^{2+}, Cd^{2+} and Cr^{3+}) with higher concentration in the samples collected from the inlets of metallic mine wastewater in Poyang Lake valley. Considering that the wastewater has been treated before the emission, the trace amount of the five ions in our tests was selected according to their maximum allowable emission concentration (Table 1). So the initial concentration of Cu^{2+}, Zn^{2+}, Pb^{2+}, Cd^{2+} and Cr^{3+} in the mixed solution was set to 5, 5, 1, 1 and 1 mg·L^{-1}, respectively.

To gain the experimental maximum removal amount of DTCR for the five metal ions at room temperature, the removal equilibrium experiments were performed under the optimized operating conditions of DTCR, and there was only one kind of metal ion in the aqueous phase. To reach the removal equilibrium fully and quickly, the initial concentration of the single ion was selected to 50 mg▪Λ^{-1}.

The stock solutions (1000 mg▪Λ^{-1}) used in the experiments were prepared by dissolving appropriate amounts of nitrate salts of Cu^{2+}, Zn^{2+}, Pb^{2+}, Cd^{2+} and Cr^{3+} in deionized water. The working solutions were prepared by diluting the stock solutions. The chemicals and regents supplied by Sigma-Aldrich were all analytical grades and used without any further purification. Adjustment of pH was accomplished by using 0.1 mol· L^{-1} NaOH and HNO_3. Distilled water was used throughout this work.

2.2. Chelating performance tests of DTCR

Static experiments were employed to determine the removal performance of DTCR. The tests were carried out by shaking 150 mL of simulated solution with a desired pH into a conical flask. Then a certain amount of DTCR was added and the resulting suspension was instantly stirred at 400 rpm under the setting temperature. Subsequently, the samples were taken at predetermined time intervals and centrifuged at 4000 rpm for 2 min. The concentration of residual heavy metals in the supernatant was analyzed. Moreover, the suspended sediment in the treated samples, namely the chelating product of DTCR, was collected by the centrifugation and dried into powder to be used in the following structural characterization.

The removal efficiency of every metal ion was determined by using the following Eq. (1), where $C_{i, M}$ and $C_{f, M}$ (mg·L^{-1}) represent the initial and final concentrations of metal ion M in the aqueous phase, respectively, and M represents Cu^{2+}, Zn^{2+}, Pb^{2+}, Cd^{2+} and Cr^{3+}, respectively.

Table 1
Part of emission concentration of toxic metal ions in national integrated wastewater discharge standard in China [2]

Toxic metal ions	Maximum allowable emission concentration (mg/L)
Cu^{2+}	1.0
Zn^{2+}	5.0
Pb^{2+}	1.0
Cd^{2+}	0.1
Cr^{3+}	1.0

$$\text{Removal efficiency M (\%)} = (C_{\text{i, M}} - C_{\text{f, M}}) \times 100\%/C_{\text{i, M}} \quad (1)$$

The maximum removal amount of every metal ion on DTCR was calculated by Eq. (2), where $Q_{e,\,M}$ (mmol·g⁻¹) is the removal amount of metal ion M on per unit mass of DTCR after the equilibrium, $C_{0,\,M}$ and $C_{e,\,M}$ (mmol·L⁻¹) represents the initial and equilibrium concentrations of metal ion M in the aqueous phase, respectively. V (L) is the volume of aqueous phase, W (g) is the dry weight of the chelating agent used in the test, and M represents Cu^{2+}, Zn^{2+}, Pb^{2+}, Cd^{2+} and Cr^{3+}, respectively.

$$Q_{\text{e, M}} = (C_{\text{0, M}} - C_{\text{e, M}}) \times V/W \quad (2)$$

It should be noted that the chelating agent DTCR utilized in this part should be diluted 100 times by volume before the application, since the initial content of every investigated metal ion was trace amount in the investigated systems.

2.3. Characterization and instrumentation

An inductively coupled plasma atomic emission spectrometry (ICP-AES, Optima-2100DV, and Perkin Elmer of US) was used to measure the concentrations of metal ions. The detection limits of this equipment for metal ion concentration are lower than 0.001 mg·Λ⁻¹ and it can detect multiple metal ions simultaneously. The pH measurements were performed by using a pH meter (PHS-3C, Shanghai Precision Instrument Factory, China) equipped with a combined pH electrode.

The aqueous solution of DTCR (volume fraction 1‰) was prepared and scanned at 220–420 nm with an ultraviolet spectrophotometer (UR, TU-1901, Beijing Purkinje General Instrument Co., Ltd. China) for the initial confirmation of the functional groups. Moreover, the dried samples of DTCR and its chelating products with the single metal ion were grinded into fine powder to press into tablets with KBr. The spectra of the tablets were scanned at 4000–400 cm⁻¹ with a Fourier transform infrared spectrometer (FT-IR, Nicolet 6700, Thermo Nicolet of US). The data were analyzed to determine the functional groups and their chemical shifts before and after adsorbing different single metal ion. Elemental analysis was carried out by TCH600 Nitrogen/Oxygen/Hydrogen Determinator and SC600 Carbon/Sulfur Determinator (LECO Co., USA). The surface chemical compositions as well as the surface morphologies of DTCR before and after adsorbing metal ions were analyzed by X-ray Photoelectron Spectrometer (XPS, ESCALAB 250Xi, Thermo Fisher Scientific of UK) and Scanning Electron microscope (SEM, Quanta200F, FEI Co., USA), respectively. The computer deconvolution was applied to detect the elemental peaks of N, S and metal ions present in samples.

2.4. Computational details for removal mechanism study

Density functional theory (DFT) has been proved to be computationally efficient for providing valuable information about the removal mechanism of metal ions on adsorption materials. It can be used to evaluate the degree of distortion and interaction between metal ions and functional groups of the chelating agent. Moreover, the binding energy of the metal ion on different functional group could be calculated to further compare the difference in the removal mechanism of different metal ion on DTCR. So all the quantum chemical calculations in this work were based on DFT and carried out by using the Gaussian 03 suit of programs [24].

Geometries of DTCR model and its metal complexes were all fully optimized by DFT method with the B3LYP hybrid density functional theory. The C, N, S and H atoms used the basis set of 6-311++G(2df, 2p), while the metal ions were depicted by LANL2DZ which is a kind of pseudopotential basis set to calculate transition-metal ligands credibly [23,25,26]. All the possible geometries were fully optimized without any symmetry constraints. The ultrafine integration grid was used to ensure the convergence of calculation. Additionally, vibration frequencies were calculated at the same level of optimization to identify the nature of stationary points and obtain zero-point-energy (ZPE) corrections. The related energies were all obtained by single point energy calculations at the level of B3LYP/6-311++G(2df, 2p) (LANL2DZ for metal ions), and the solvent effect of water was also estimated by the polarizable continuum model to add the further relevance to the removal process [27].

3. Results and discussion

3.1. Removal performance of DTCR in metallic mine wastewater

3.1.1. Effect of DTCR dosage

The effect of DTCR dosage on the removal in mixed solutions was studied at room temperature (25°C) with 150 mL mixed metal ions solution (original pH ≈ 5.5) and the interaction time was 20 min. The initial concentration of every metal ion was consistent with Section 2.1. The relation between the removal efficiency of every metal ion and the amount of DTCR dilution is shown in Fig. 1. The optimum dosage range for the removal of the five metal ions in 150 mL mixed solution was 1.4–1.6 mL of DTCR dilution. The data in Fig. 1 also indicate that the removal rate of the five metals was not always increased with the increase in DTCR dosage. All the removal rates would be decreased obviously when the excessive amount of DTCR was added. This might be caused by the good solubility of DTCR. The excess agent could dissolve some of the chelating products, which would make the residual amount of metal ions in the treated water increase. Furthermore, there existed a competitive adsorption between the five ions in the mixed solution for the functional groups of DTCR, when the dosage of the chelating agent was not enough (for example 0.6–0.8 mL). The competition among the five ions for the functional groups of DTCR followed the order of $Cr^{3+}>Cu^{2+}>Pb^{2+}>Zn^{2+}>Cd^{2+}$.

3.1.2. Effect of initial pH

To gain the effect of initial pH value on the removal efficiency, the dosage of DTCR was the optimized in Section 3.1.1, and the pH value of mixed solution was varied from 3 to 11, while other experimental conditions were kept constant. The effect of initial pH value on the removal rates of different metal ions in the mixed solution is presented in Fig. 2. It indicated that in the mixed solution, the removal

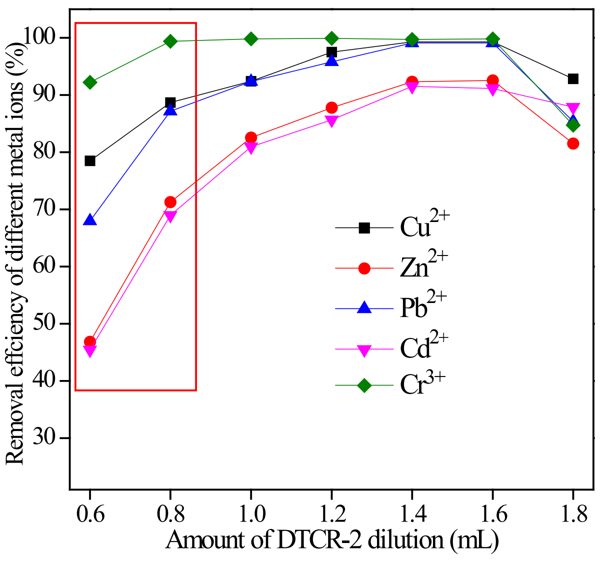

Fig. 1. Effect of DTCR dosage on the removal efficiency of every metal ion in mixed solution.

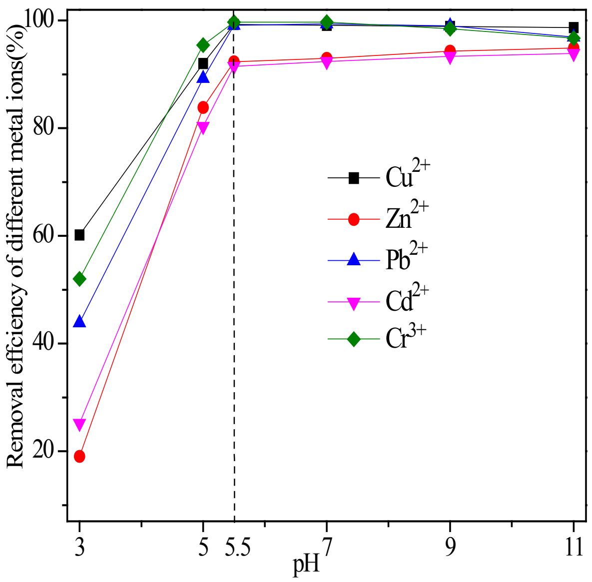

Fig. 2. Effect of initial pH value on the removal efficiency of every metal ion in mixed solution.

rate of every ion was greatly affected by the pH value when it was lower than 5. But when it was higher than 5.5, almost all the removal rates of the metal ions attached the maximum and became stable, which meant that there was a wide pH range (>5.5) of the DTCR application and the strongly basic conditions had a little impact on the removal capacity of DTCR. When the pH value was 5.5, the maximum removal rate of Cr^{3+}, Cu^{2+}, Pb^{2+}, Zn^{2+} and Cd^{2+} was 99.70%, 99.28%, 99.10%, 92.33% and 91.49%, respectively, and the residual concentration of the five metal ions in the treated water was 0.003, 0.036, 0.009, 0.383 and 0.085 mg/L. Given that the original pH value of the metallic mine wastewater was about 5.5, it seemed that DTCR had a promising prospect for the application in the deep treatment of metallic wastewater with weak acidity. Moreover, the experimental result proved that the dosage of DTCR in this work had little effect on the initial pH value under the operating conditions.

3.1.3. Effect of time and initial concentration

To investigate the effect of time and initial concentration on the removal performance of DTCR, the study was carried out with different initial concentration of ions, while the dosage of DTCR and the initial pH value were optimized. The other operating conditions were kept constant. Taking into account that the concentrations of the five metal ions in effluents should be lower than the discharged standard, the initial concentrations were selected as shown in Fig. 3. It shows that all the removal efficiencies of the five metals in mixed solutions were increased with removal time. No matter how much the initial concentration was, the removal process would reach the equilibrium after 20 min, while the equilibrium time for the low concentration was about 10 min (Fig. 3b). This might be caused by the rapid and complete adsorption at a relatively low initial concentration. Additionally, as shown in Fig. 3b, there was a little decrease in the removal rates of the five metal ions when the adsorption time was longer than 30 min. This might also be caused by the solubility of DTCR. Because that the dosage of DTCR might be excessive compared with the system with relatively lower initial concentration of metal ions. With the prolongation of adsorption time, the excessive DTCR would dissolve the chelating complexes and the removal efficiency would be reduced.

3.1.4. Effect of temperature

The removal rates of various ions in the mixed solution at different temperature are illustrated in Fig. 4. It displays that with the increase of temperature, the removal rate of the five ions could raised slowly. When the temperature was higher than 40°C, the removal rate decreased, especially Cd^{2+} and Zn^{2+}. The possible reason was the removal process might be exothermic reaction, which could occur spontaneously at room temperature. The higher temperature would inhibit the reaction [28].

The above experimental results implied that when the removal time was longer than 20 min and the temperature was in the range of 10–40°C, the effect of these factors on the removal would be very little. Considering of the economic benefit, the process of wastewater treatment should be as convenient as possible. So the optimized operating conditions of DTCR were the volume ratio of DTCR to wastewater about $1:10^4$, pH ≈ 5.5, removal time 20 min and ambient temperature (25°C). Under the optimized conditions, the removal rate of Cr^{3+}, Cu^{2+}, Pb^{2+}, Zn^{2+} and Cd^{2+} in the treated water could reach 99.70%, 99.28%, 99.10%, 92.33% and 91.49%, respectively, and the residual content of the five ions were 0.003, 0.036, 0.009, 0.383 and 0.085 mg/L. By comparison with Table 1, the residual content of Cr^{3+}, Cu^{2+} and Pb^{2+} were obviously lower than the required in the emission standard, while the residual concentration of Zn^{2+} and Cd^{2+} was relatively high, especially of Cd^{2+}. It meant

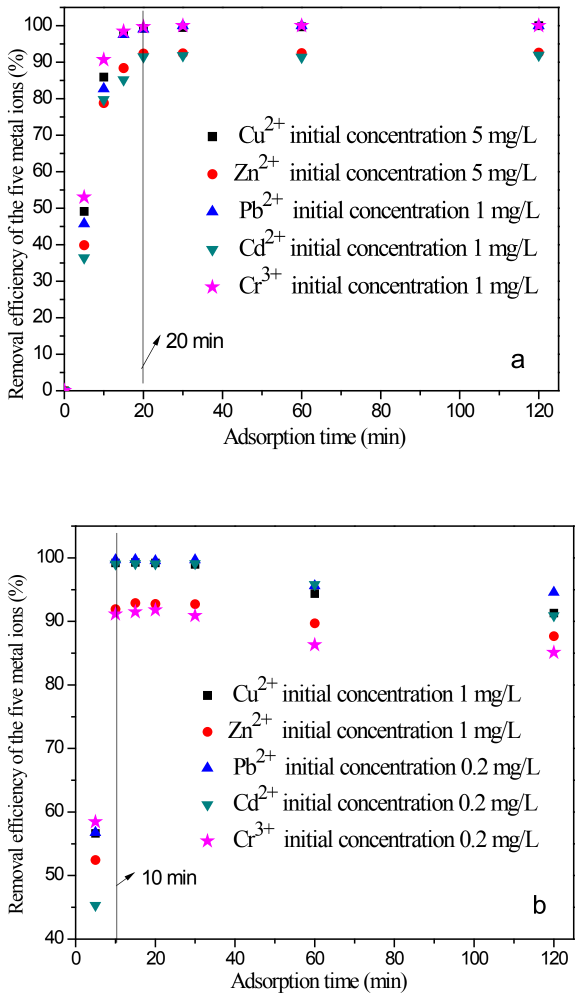

Fig. 3. Effect of time and initial concentration on the removal efficiency of every metal ion in mixed solution, (a) relatively higher initial concentration, (b) relatively low initial concentration.

that the available DTCR was poor for removing Zn^{2+} and Cd^{2+} effectively from the mixed solution with trace amount of metal ions.

3.1.5. Experimental removal capacity of DTCR for different ion at equilibrium

To determine the experimental removal capacity of DTCR for the five metal ions after the equilibrium at ambient temperature (25°C), the removal capacity of the five ions in the single solution was measured as a function of contact time under the optimized operating conditions, and the results are presented in Fig. 5.

As displayed in Fig. 5, there were all rapid uptake kinetics and removal equilibrium for the five metal ions, which would be attained within 20 min. To ensure the equilibrium conditions were all achieved, the contact time was investigated until 480 min, and the experimental removal capacity of DTCR for every metal ion had no further changed when the contact time was longer than 30 min. The experimental removal capacity of DTCR for Cr^{3+}, Cu^{2+}, Pb^{2+}, Zn^{2+} and Cd^{2+} could reach to 2.16 mmol· g^{-1}, 1.18 mmol· g^{-1}, 1.13 mmol· g^{-1}, 0.58 mmol· g^{-1} and 0.55 mmol· g^{-1} after the equilibrium, respectively, when the initial concentration of every metal ion was 50 mg·Λ^{-1} and the weight of DTCR in the form of dry powder was about 0.0169 g. These experimental data about the removal capacity of DTCR would be helpful to verify the accuracy of related theoretical calculation about the removal mechanisms of DTCR for the five metal ions in the following section.

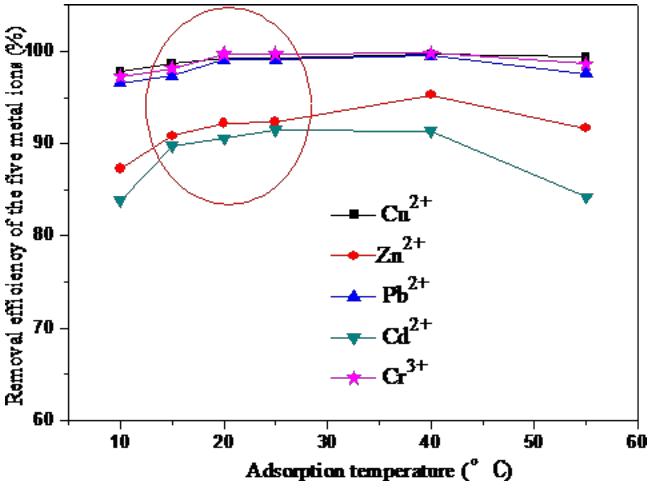

Fig. 4. Effect of temperature on the removal efficiency of every metal ion in mixed solution.

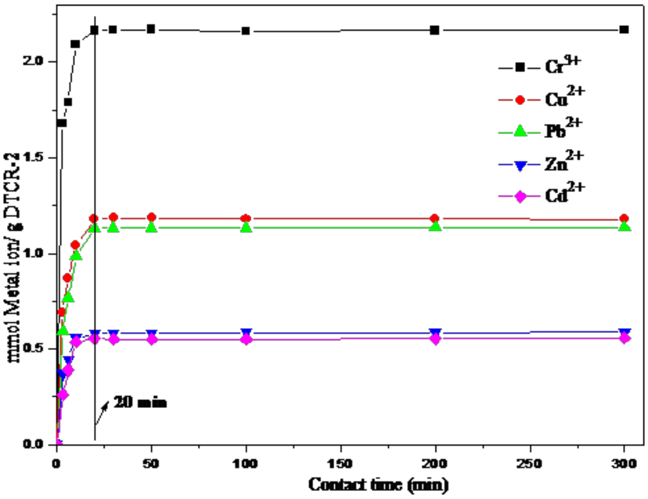

Fig. 5. Adsorption rate of every metal ion on DTCR (initial concentration C_0 in the simulated wastewater with single metal ion was 50 mg/L, pH = 5.5, temperature was 25°C).

3.2. Characterization for DTCR and its chelating products

3.2.1. UVS

The dilution of DTCR was scanned by an ultraviolet spectrophotometer (UVS), and the ultraviolet spectrum of

DTCR is displayed in Fig. 6. The analysis indicated that there were two kinds of absorption peaks. The one occurred at the vicinity of 230 nm was attribute to π-π* transition of N···C···S groups and the other at 286 nm was attribute to n-π* transition of the non-bonding electron on sulfur atoms to the conjugated system in S···C···S groups [29]. There would be two kinds of characteristic bonds in the structure, one was between atoms of C and N with lone pair electrons, and the other was between atoms of C and S with double bond. So the major functional groups in DTCR were –N-CS_2 included bonds of C=S and C-N.

3.2.2. FT-IR

The FT-IR spectra are given in Fig. 7. A large broad band near 3412 cm^{-1} was probably attributed to the presence of the stretching vibrations of N-H in functional groups [28,30]. The characteristic absorption peaks appearing at 1434 cm^{-1}, 1148 cm^{-1} and 620 cm^{-1} were attributed to the vibration of N-CS_2, C=S and C-S, respectively. This further proved that there were dithiocarbamate (DTC) groups in DTCR. Compared with the spectrum of DTCR, the vibration frequencies of C=S and C-S in DTC-M (M=Cu, Zn, Pb, Cd, Cr) were all deviated from 1148 cm^{-1} and 620 cm^{-1}. The absorption peaks of N-H stretching in 3412 cm^{-1} were also widened and shifted in DTC-Cr, DTC-Pb and DTC-Cu, and only the characteristic absorption peak of N-C=S was not observed from the FT-IR spectrum of DTC-Cr. The comparison indicated that all the five metal ions could be captured by a strong metal-ligand bond formed between the metal ion and the functional group of C=S or C-S in DTCR. Furthermore, the chelating capability between Cr^{3+}, Pb^{2+}, Cu^{2+} and DTCR would be enhanced, since the three metal ions could be adsorbed by the isolated pairs of electron on the group of -NH-. Moreover, Cr^{3+} with the strongest alkali could also interact with N on the group of N-CS_2 by the coordination of isolated pairs of electron on N. So the chelating selectivity of DTCR for different metal ions was diverse.

3.2.3. XPS

The XPS spectra of DTCR before and after removing different metal ions (DTC-M) are displayed in Fig. 8. All the elements (except of H atoms) contained in DTCR and DTC-M could be reflected in the spectra, which indicated that there were no oxygen atoms in DTCR, and the molecule of DTCR was composed of C, N and S atoms. The element of Na was contained in DTCR, but the element was not detected in DTC-M (M = Cu, Zn, Pb, Cd and Cr). Because that the Na^+ was completely replaced by the adsorbed metal ions. In order to clarify the removal mechanism of the five metal ions on DTCR, the XPS analyses for DTCR and different ion on DTCR are shown in Figs. 9–11.

3.2.3.1. XPS results of DTCR and DTC-Cr

The high resolution core-level spectra of S_{2p} and N_{1s} of DTCR and DTC-Cr resolved into individual component peaks are displayed in Fig. 9. The S_{2p} binding energies of C=S bond (peak 1 in Fig. 9a), C-S bond (peak 2 and 3 in Fig. 9a) in DTC groups of DTCR were 160.93 eV, 161.78 eV

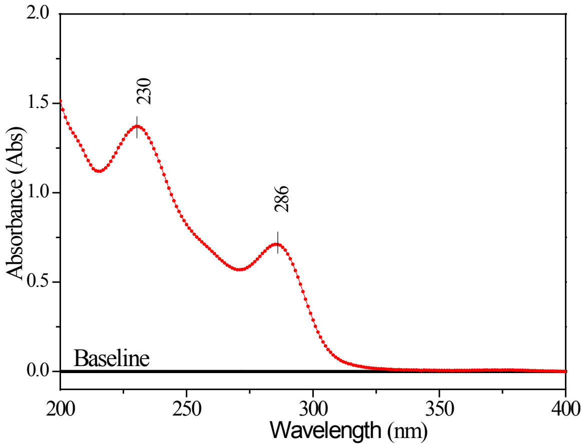

Fig. 6. Ultraviolet spectrogram of chelating agent DTCR.

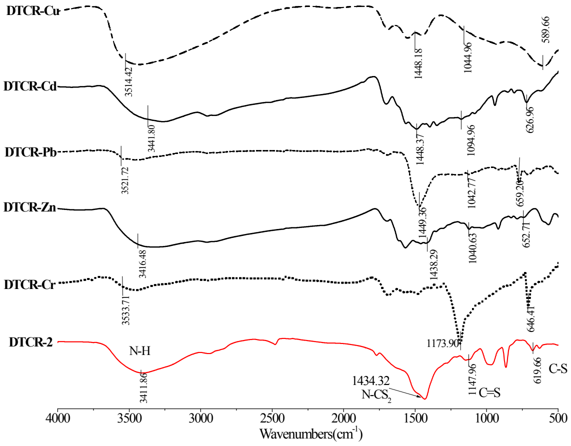

Fig. 7. FT-IR spectra of DTCR and its chelating product with single metal ion DTCR-M (M= Cu, Zn, Pb, Cd and Cr).

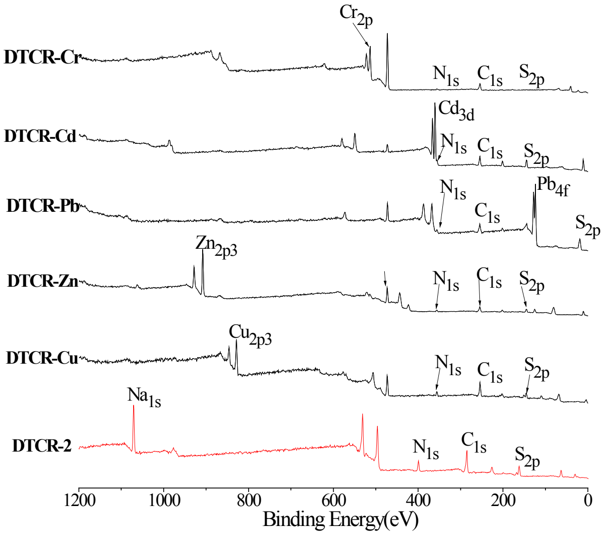

Fig. 8. XPS spectra of DTCR and its chelating product with single metal ion DTCR-M (M= Cu, Zn, Pb, Cd and Cr).

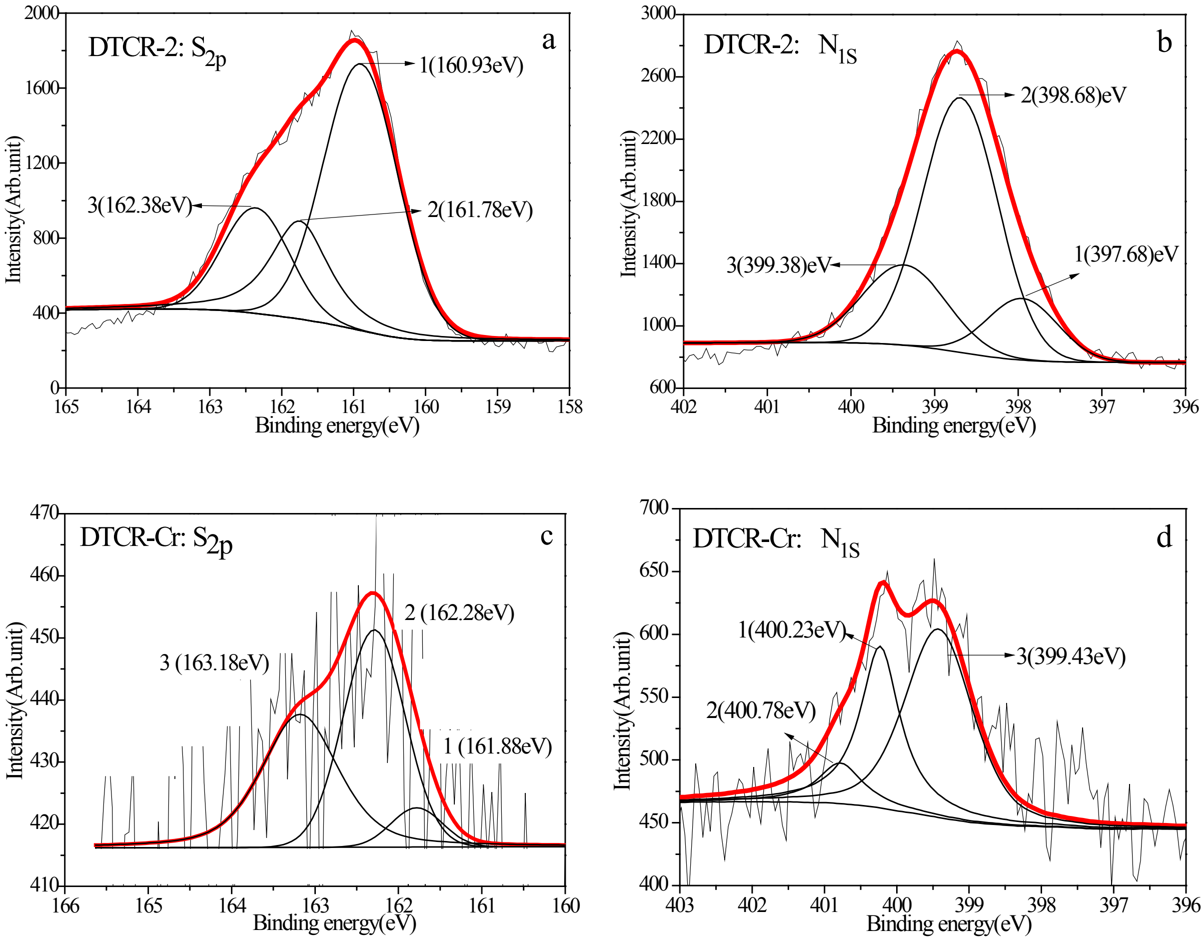

Fig. 9. The high-resolution core-level spectra of S_{2p} and N_{1s} for chelating agent DTCR (a, b) and chelating product DTC-Cr (c, d).

and 162.38 eV, respectively. By contrast, the same binding energies of C=S and C-S bond in DTC groups of DTC-Cr (peak 1, 2 and 3 in Fig. 9c) were 161.88 eV, 162.28 eV and 163.18 eV, respectively. The binding energies of C=S and C-S bonds in DTC group of DTC-Cr were all a little higher than those in DTCR, which resulted from the donation of electrons from S atoms of C-S and C=S in DTC groups to Cr^{3+} [31]. It indicated that there might exist chelating bonds formed between Cr^{3+} and the bonds of C-S and C=S in DTCR.

The N_{1s} binding energies of -NH-/-NH_2 in DTCR before and after chelating Cr^{3+} were 397.68 eV in peak 1 of Fig. 9b and 400.23 eV in peak 1 of Fig. 9d, respectively. The N_{1s} binding energies of the groups in DTC-Cr was much higher than those in DTCR, which was caused by the donation of lone pair electrons on N atom to the shared bond between the N atom on –NH-/-NH_2 and Cr^{3+} [32]. As a result, a complex between Cr^{3+} and N atom in group of -NH-/NH_2 in DTCR was formed, and the electron cloud density in this N atom was decreased [33]. Moreover, the peak 2 at 400.78 eV in Fig. 9d was corresponding to the group of N-CS_2 in DTC-Cr, whose N_{1s} bonding energy was increased about 2.1 eV after the adsorption of Cr^{3+} compared with that in peak 2 of Fig. 9b, since the electrons transferred from N atom on the N-CS_2 group to Cr^{3+} and a coordination bond between Cr^{3+} and N atom on the group was formed. The N_{1s} binding energies of –NR_2 in DTCR and DTC-Cr were 399.38 eV in peak 3 of Fig. 9b and 399.43 eV in peak 3 of Fig. 9d, respectively, which proved that there was no interaction between Cr^{3+} and -NR_2, since there was no obvious change in N_{1s} binding energies of -NR_2 after the removal.

3.2.3.2. XPS results of DTC-Cu and DTC-Pb

The S_{2p} binding energies of C=S bond in DTCR and DTC-Cu were 160.93 eV and 161.98 eV (peak 1 in Fig. 9a and 10a), respectively. The peaks 2 and 3 at 161.78 eV and 162.38 eV in Fig. 9a, as well as those at 162.73 eV and 163.08 eV in Fig. 10a were attributed to C-S bonds in DTCR and DTC-Cu, respectively. The comparison between the three peaks in Fig. 9a and 10a, indicated that there were small changes in the binding energies of C-S/C=S after chelating Cu^{2+}, and there also existed the donation of electrons from S atoms on bonds of C-S/C=S to Cu^{2+}. The above interaction between Cu^{2+} and C-S/C=S was identical to that of Cr^{3+}, which also meant that there were chelating interaction between Cu^{2+} and C-S/C=S. The N_{1s} binding energies of -NH-/NH_2 (peak 1), N-CS_2 (peak 2) and -NR_2 in DTC-Cu

(Fig. 10b) were 400.43, 398.62 and 399.31 eV, respectively. By the comparison with those energies in DTCR (Fig. 9b), the result indicated that only -NH-/NH_2 in the nitrogenous groups of DTCR could form complexes with Cu^{2+}.

The S_{2p} and N_{1s} analysis of DTC-Pb (presented in Figs. 10c and 10d) was almost consistent with those of DTC-Cu, which implied that the chelating mechanism of DTCR for Pb^{2+} was similar to that for Cu^{2+}.

3.2.3.3. XPS results of DTC-Zn and DTC-Cd

The analysis about the binding energies of S_{2p} and N_{1s} in Fig. 11 indicates that the chelating mechanisms of DTCR for Zn^{2+} and Cd^{2+} were the same. The comparison of S_{2p} binding energies in Figs. 9a, 11a and 11c demonstrates that both Zn^{2+} and Cd^{2+} could be chelated by the C=S/C-S bonds in the DTC group of DTCR, which was similar to the chelating interaction between DTCR and Cu^{2+}, Pb^{2+} and Cr^{3+}. However, the N_{1s} binding energies of all the three kinds of nitrogenous groups in DTC-Zn/Cd were almost the same with those in DTCR by comparing Figs. 9b, 11b and 11d, which demonstrate that there were no interaction between all the nitrogenous groups in DTCR and the metal ions of Zn^{2+} or Cd^{2+}.

3.2.4. SEM and elemental analysis

The surface morphological changes of DTCR before and after chelating mixed heavy metal ions were clearly seen in SEM micro photographs of Figs. 12a and 12b. As shown in Fig. 12a, DTCR had a compact structure and a rough surface with obvious concavo-convex shape. Such a polymer structure would be more conductive to capturing heavy metal ions [34]. On the contrary, the structure of chelating product of DTCR with heavy metal ions became much tighter and its surface was relatively smoother, since the cracks on the surface of DTCR were packed into blocks. The changes in the surface morphologies of DTCR before and after the chelating further indicated that there existed interaction between DTCR and mixed metal ions.

Elemental analysis results confirmed that there were only four kinds of elements in DTCR, which contained 62.43 wt% of C, 27.64 wt% of H, 2.70 wt% of N and 7.23 wt% of S. It could be calculated that there were 1.93 mmol· g^{-1} of N-containing groups as well as 2.26 mmol· g^{-1} of S-containing groups in DTCR. The molar ratio of N/S in DTCR was higher than 1:2. Combined with the results of UVS, FT-IR and XPS for the functional group structure of DTCR, it demonstrated that there were 1.13 mmol· g^{-1} of DTC groups (-NCS_2) in DTCR and 0.80 mmol· g^{-1} of other amino

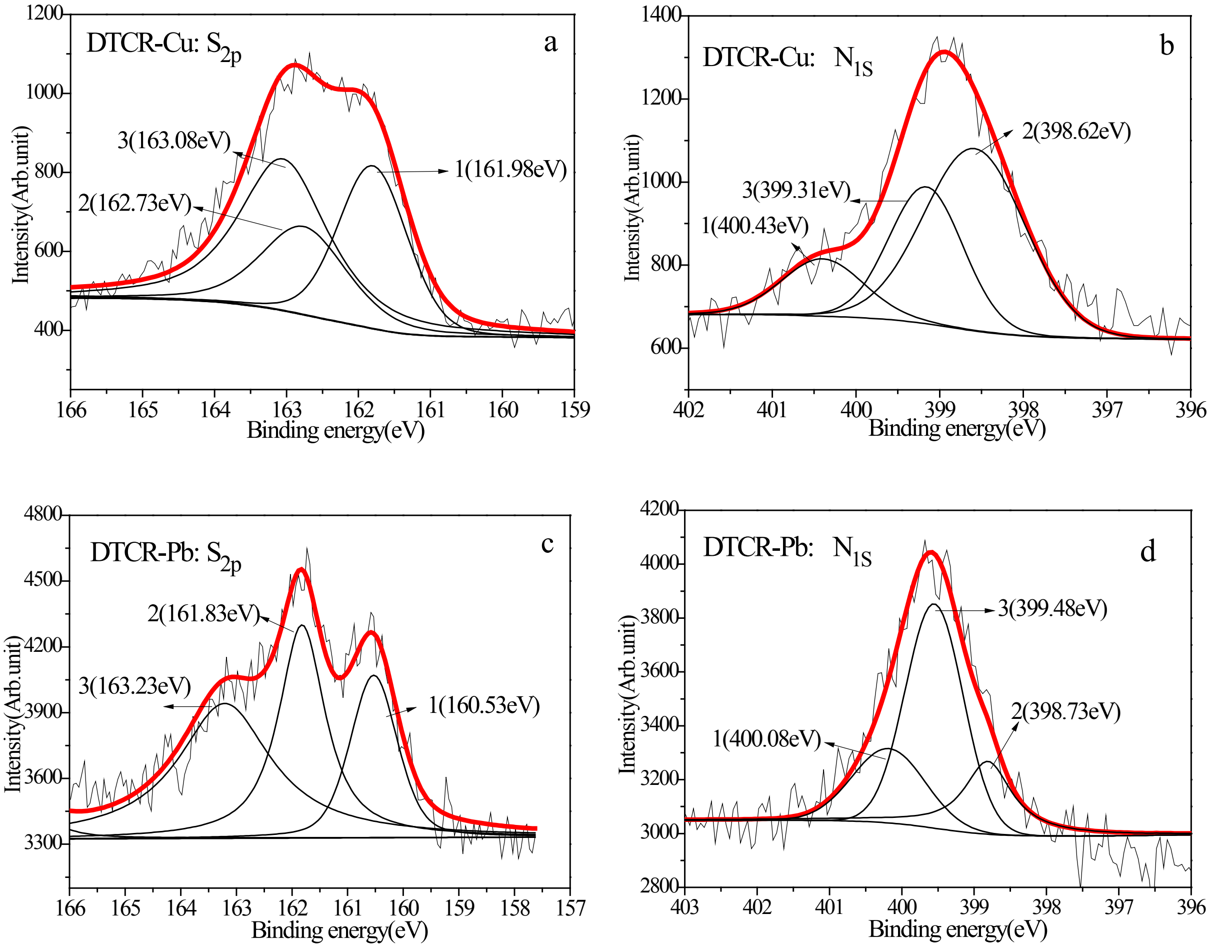

Fig. 10. The high-resolution core-level spectra of S2p and N1s for chelating product DTC-Cu (a, b) and DTC-Pb (c, d).

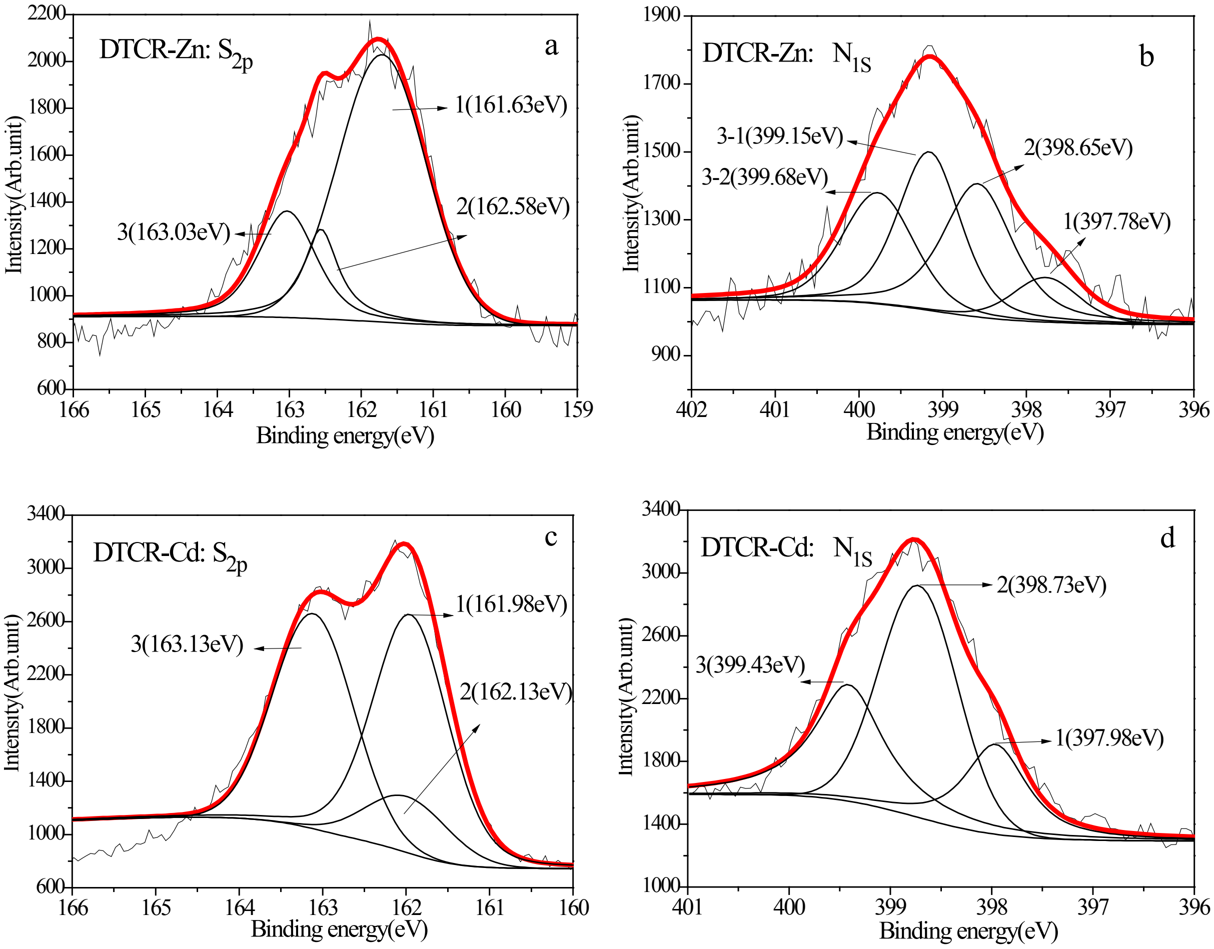

Fig. 11. The high-resolution core-level spectra of S2p and N1s for chelating product DTCR-Zn (a, b) and DTCR-Cd (c, d).

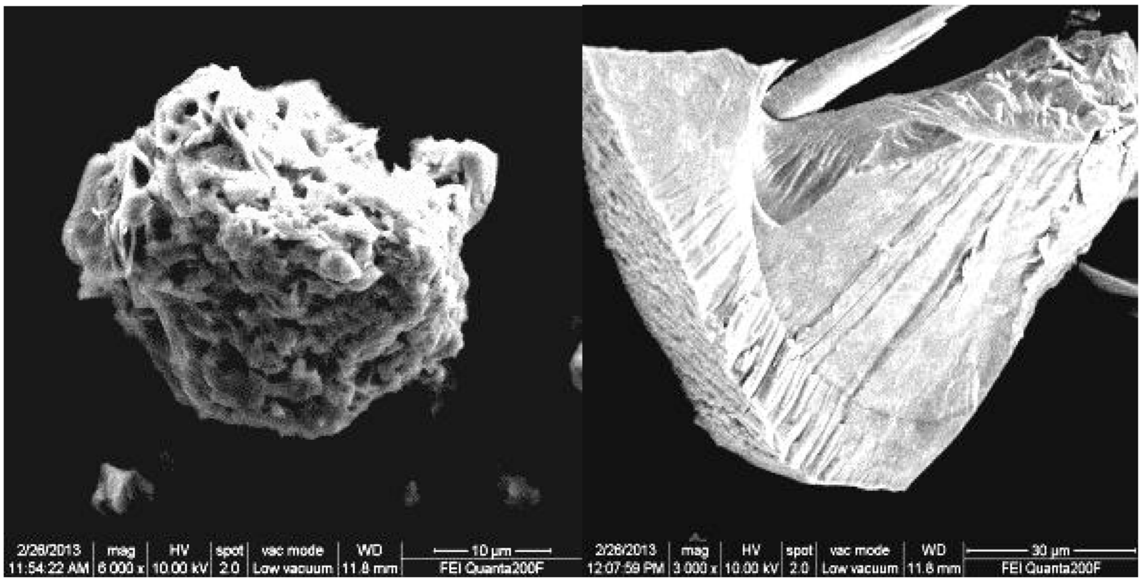

Fig. 12. Scanning electro microphotograph of (a) DTCR and (b) chelating product of DTCR with mixed heavy metal ions.

groups (-NH-, -NH_2 or -NR_2) which were not on the DTC groups.

The characterization results in Section 3.2 revealed that there was no oxygen atom in DTCR molecule. The major functional groups in DTCR were DTC groups (-NCS_2) and amino groups (-NH-, -NH_2 or -NR_2) which were not on the DTC groups, whose content were 1.13 mmol· g^{-1} and 0.80 mmol· g^{-1}, respectively. So the major functional groups contained in DTCR are displayed in Fig. 13.

The characterization results in Section 3.2 indicated that all the five ions could be captured by the metal-ligand bond formed between metal ions and C=S/C-S on the DTC groups, while could not be interacted with –NR_2 either on DTC groups or not. But the interaction ability between Cr^{3+}, Pb^{2+}, Cu^{2+} and DTCR could be enhanced by the donation of isolated pairs of electrons in N atom of -NH_2 and -NH- which were not on DTC groups to form the shared bond between N atom and the three metal ions. These results were similar with the reported removal mechanism of Bai et al. [28]. Besides, Cr^{3+} could be further attracted by the N atom on the DTC group (N-CS_2) with the help of isolated electron pairs in N atom. The above interactions between the different functional groups of DTCR and metal ions are summarized in Table 2.

3.3. Theoretical calculation about removal mechanism of DTCR for metal ions

DFT method was employed to further explore the possible removal mechanism of different single metal ion on the active sites of DTCR at the molecular level, and the related calculations were carried out based on detailed methods in Section 2.4.

Since the characterization in Section 3.2 had proved the major functional groups in DTCR (Fig. 13), the computational manageable cluster model shown in Fig. 14a which contains these typical groups was constructed and used to represent DTCR molecule for the cost-effective calculation. In Fig. 14a, the groups of [-N1H1-C1S1S3] and [-N2(CH_3)-C2S2S4] were the DTC groups in the cluster model, and the electric charge of the cluster model was –2. It should be noted that the groups of -N1H1- and -N2R_2 were the secondary and tertiary amine group on the DTC groups, respectively. By contrast, -N3H2- (-N4H3-), -N5R_2 (-N6R_2) and -N7H4H5 (-N8H6H7) were the secondary, tertiary and primary amines which were not on DTC groups, respectively. Although the cluster model could not accurately represent the whole environment of the chelating agent, it was particularly suited to describe local phenomena such as the interaction between adsorbents and active sites of adsorption agents as well as the new bonds forming calculated by high-quality theoretical methods. Calculations with such cluster models had been proved to be adequate for qualitative descriptions of chemical rearrangements that occur locally on active sites [23,25]. In addition, our calculation purpose was to study the difference in the removal property of DTCR for the five metal ions, and the investigated energies were relative, so the cluster model could make the reasonable estimates for the calculation.

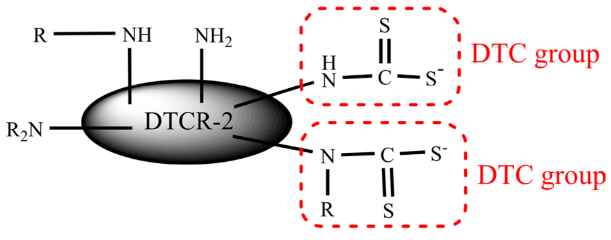

Fig. 13. Scheme of major functional group of DTCR based on characterization analysis.

Table 2
Characterization results about the interaction between functional groups of DTCR and different metal ions

Functional bonds	Different meal ions (√: presence of interaction; ×: no presence of interaction)				
	Cu^{2+}	Zn^{2+}	Pb^{2+}	Cd^{2+}	Cr^{3+}
C=S/C-S **on** DTC groups	√	√	√	√	√
-NH-/-NH_2 **not on** DTC groups	√	×	√	×	√
-NH- **on** DTC groups	×	×	×	×	√
-NR_2 **on or not on** DTC groups	×	×	×	×	×

The optimized geometric structures of DTCR cluster before and after trapping different single metal ion are shown in Fig. 14, and the related main structural parameters are tabulated in Table 3. The structures in Fig. 14 combined with the parameters in Table 3 demonstrate that geometrical changes in the DTCR cluster were mainly due to the presence of different metal ions, and the configurations of these metal complexes were variable according to the adsorption sites of metal ions.

For example, as shown in Fig. 14b and Table 3, there were metal-ligand bonds formed between S atoms on DTC groups and M (M= Cu^{2+}, Cr^{3+}, Zn^{2+}, Pb^{2+} and Cd^{2+}) in the metal complex, as all the bond lengths of M-S1, M-S2, M-S3 and M-S4 were in the ranges of 0.221–0.253 nm, which were all slightly longer than the sum of covalent radius of M-S. The sum of covalent radius of Cu-S, Cr-S, Zn-S, Pb-S and Cd-S was 0.219, 0.220, 0.227, 0.249 and 0.250 nm, respectively [35]. Meanwhile, the bonds of C=S in the two DTC groups were visibly elongated at least 0.002 nm while the bonds of C-S and C-N on DTC groups were shortened about 0.009 nm, and the two bond angles (S1C1S3 and S2C2S4) became smaller after the chelating adsorption. This calculation result was similar to the study of Bala subramaniam on the removal mechanism of DTC groups for Ni^{2+} [36]. It indicated that all the five metal ions could be captured by the coordination of C=S/C-S bonds on DTC groups, as a kind of chelating complex was constructed by one metal ion and two DTC groups [28].

The optimized complex structures in Fig. 14c and 14d proved that three kinds of investigated metal ions (Cr^{3+}, Cu^{2+} and Pb^{2+}) could also form the coordinate bonds with the N atom of -NH_2 and -NH- which were not on the DTC groups [23], since the new coordination bond lengths in

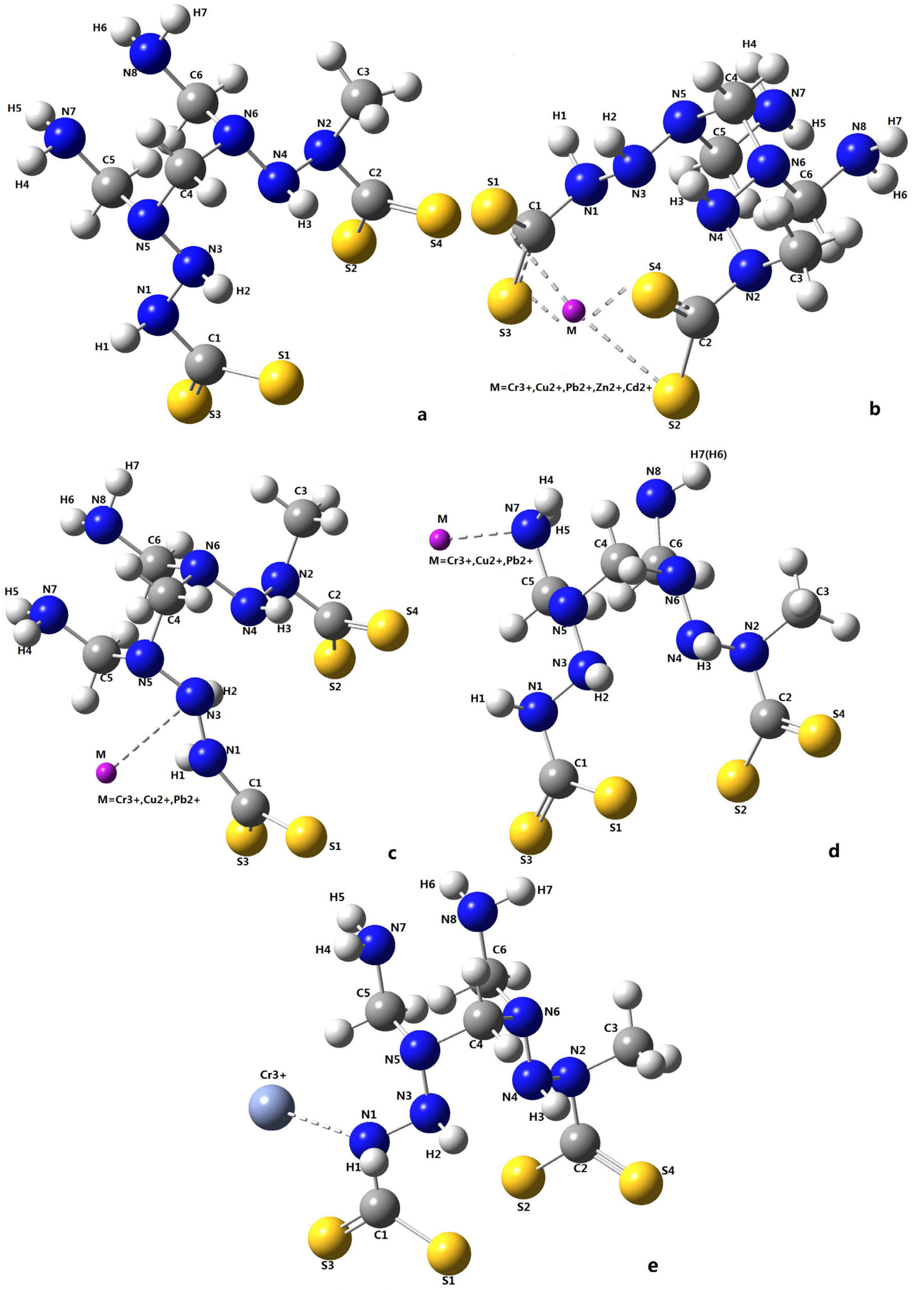

Fig. 14. Optimized structures of DTCR cluster before and after chelating single metal ion with different functional group, (a) optimized structure of DTCR cluster, (b) complex structures of Cr^{3+}, Cu^{2+}, Pb^{2+}, Zn^{2+}, Cd^{2+} coordinated by C=S/C-S on DTC groups of DTCR, (c) and (d) complex structures of Cr^{3+}, Cu^{2+}, Pb^{2+} coordinated by –NH2 and –NH– not on DTC groups of DTCR, (e) complex structures of Cr^{3+} coordinated by –NH– on the DTC group of DTCR.

Table 3
Important geometric characteristics for optimized structures of different metal ion captured by various functional groups in cluster of DTCR in Fig. 14

Materials and status	Distance of two atoms (nm), bond angles of three atoms (°) and dihedral angles of four atoms (°)											
Interact with C=S/ C-S on DTC groups	C1S1	C1S3	C2S2	C2S4	C1N1	C2N2	MS1	MS2	MS3	MS4	S1C1S3	S2C2S4
[DTCR]$^{2-}$ (Fig. 14a)	0.1782	0.1701	0.1783	0.1711	0.1390	0.1393	–	–	–	–	120.52	121.04
[DTCR-Cr]$^{+}$ (Fig. 14b)	0.1702	0.1751	0.1716	0.1750	0.1299	0.1305	0.2239	0.2242	0.2291	0.2279	110.18	112.50
[DTCR-Cu] (Fig. 14b)	0.1711	0.1744	0.1713	0.1748	0.1312	0.1319	0.2217	0.2215	0.2297	0.2289	112.93	113.71
[DTCR-Pb] (Fig. 14b)	0.1719	0.1742	0.1721	0.1743	0.1317	0.1322	0.2509	0.2513	0.2541	0.2538	114.05	114.82
[DTCR-Zn] (Fig. 14b)	0.1725	0.1736	0.1728	0.1745	0.1315	0.1318	0.2286	0.2282	0.2385	0.2392	115.21	114.98
[DTCR-Cd] (Fig. 14b)	0.1727	0.1737	0.1730	0.1739	0.1324	0.1327	0.2518	0.2531	0.2527	0.2549	116.32	116.13
Interact with –NH– not on DTC groups	C1S1	C1S3	C2S2	C2S4	C1N1	C2N2	S1C1S3	S2C2S4	MN3	N5N3N1	H2N3N1C1	
[DTCR]$^{2-}$ (Fig. 14a)	0.1782	0.1701	0.1783	0.1711	0.1390	0.1393	120.52	121.04	–	109.47	60.08	
[DTCR-Cr]$^{+}$ (Fig. 14c)	0.1782	0.1701	0.1783	0.1711	0.1390	0.1393	120.52	121.04	0.1983	140.26	68.29	
[DTCR-Cu]$^{+}$ (Fig. 14c)	0.1782	0.1701	0.1783	0.1711	0.1390	0.1393	120.52	121.04	0.1969	143.08	63.55	
[DTCR-Pb]$^{+}$ (Fig. 14c)	0.1782	0.1701	0.1783	0.1711	0.1390	0.1393	120.52	121.04	0.2307	142.75	66.12	
Interact with –NH$_2$ not on DTC groups	C1S1	C1S3	C2S2	C2S4	C1N1	C2N2	S1C1S3	S2C2S4	MN7	N7C5N5	H4N7C5N5	
[DTCR]$^{2-}$ (Fig. 14a)	0.1782	0.1701	0.1783	0.1711	0.1390	0.1393	120.52	121.04	–	109.47	60.26	
[DTCR-Cr]$^{2+}$ (Fig. 14d)	0.1782	0.1701	0.1783	0.1711	0.1390	0.1393	120.52	121.04	0.1945	113.62	22.52	
[DTCR-Cu]$^{+}$ (Fig. 14d)	0.1782	0.1701	0.1783	0.1711	0.1390	0.1393	120.52	121.04	0.1953	117.13	23.08	
[DTCR-Pb]$^{+}$ (Fig. 14d)	0.1782	0.1701	0.1783	0.1711	0.1390	0.1393	120.52	121.04	0.2301	117.85	24.22	
Interact with –NH on DTC group	C1S1	C1S3	C2S2	C2S4	C1N1	C2N2	S1C1S3	S2C2S4	MN1	H1N1C1	S1C1N1H1	
[DTCR]$^{2-}$ (Fig. 14a)	0.1782	0.1701	0.1783	0.1711	0.1390	0.1393	120.52	121.04	–	109.47	–90.05	
[DTCR-Cr]$^{2+}$ (Fig. 14e)	0.1782	0.1701	0.1783	0.1711	0.1390	0.1393	120.52	121.04	0.1994	85.04	–52.95	

Table 3 were all a little longer than the sum of covalent radius of Cr-N, Cu-N and Pb-N (0.193, 0.192 and 0.222 nm), respectively. While there were no chelating reactions took place for the three metal ions with the N atom and the S atom on the DCT group, since there were no obvious changes in the main structural parameters of DTCR cluster, except of some changes in bond angles (N1N3N5 in Fig. 14c and N7C5N5 in Fig. 14d) and dihedral angles (H2N3N1C1 in Fig. 14c and H4N7C5N5 in Fig. 14d). These structural changes were favorable to the formation of coordination complexes in Fig. 14c and 14d. While other metal ions such as Zn^{2+} and Cd^{2+} could not be captured by the N atom of -NH_2 and -NH- which were not on the DTC groups, since the related adsorption models were also calculated but the physically meaningful structures could not be obtained in these cases.

In the same way, the calculated results also verified that there was no interaction between the five metal ions and the N atom of tertiary amino (N5, N6 and N2 in Fig. 14a either on DTC groups or not). This theoretical result was conformed to the experimental characterization in Section 3.2, namely, all the metal ions could not interact with tertiary amino groups in the DTCR cluster. The calculations about the configuration in Fig. 14e confirmed that only Cr^{3+} could be captured by secondary amino on the DTC group by forming coordination bond between the ion and N atom.

In order to confirm whether the structures of complexes in Fig. 14b-14e were stable, the frequency analysis of these configurations was carried out on the basis of structural optimization. The results showed that there was no imaginary frequency in the vibration spectrum of every complex, indicating that all the configurations of complexes were stable after the structure optimization [25]. Moreover, the adsorption energy (Δ*E*), namely the energy change in the system after the adsorption of metal ion on the special function group of DTCR, was calculated by Eq. (3) [37].

$$\Delta E = [E+ZPE]_{\text{complex of metal ion on DTCR cluster}} - E_{\text{metal ion}} - [E+ZPE]_{\text{DTCR cluster}} \quad (3)$$

where $[E+ZPE]_{\text{complex of metal ion on DTCR cluster}}$ and $[E+ZPE]_{\text{DTCR cluster}}$ are the total energy of the complex and the energy of DTCR cluster after the structure optimization as well as the zero-point vibration energy correction, respectively, and $E_{\text{metal ion}}$ is the energy of metal ion.

According to the definition of Δ*E*, the interaction strength between the metal ion and various functional groups of DTCR could be measured. The larger the absolute value of Δ*E* is, the stronger the adsorption strength will be and the more stable the complex structure will be [33]. So the corresponding adsorption energies for the formation of complex in Fig. 14 were calculated and summarized in Table 4, which further demonstrated that the four kinds of functional groups in DTCR cluster could adsorb metal ions but the adsorption types as well as the adsorbabilities of the four groups for different metal ion were distinctive.

By contrast, bonds of C=S/C-S on DTC groups possessed the largest adsorption capability, since a stable chelating complex was formed by 1 mol metal ion with 4 mol C=S/C-S on the DTC group (Fig. 14b). All the five investigated metal ions could be chelated by this kind of groups, and their adsorption energies on C=S/C-S of DTC groups was the highest compared with other functional groups (Table 4). The $-NH_2$ and -NH- which were not on DTC groups had a relatively weak adsorption capability and could not interact with Zn^{2+} and Cd^{2+}, since metal ions were adsorbed just by the coordination effect of N atom in these amine groups (Fig. 14c and 14d). The influence of coordination interaction was comparatively weaker than that of complexation and greatly affected by the steric hindrance, so all the tertiary amino (either on the DTC groups or not) with the largest steric hindrance could not coordinate with any investigated ions. In addition, the coordination performance of the secondary N atom on the DTC group was greatly weakened by the chelating competition as well as the steric hindrance of C=S/C-S bonds on the DTC group. Only Cr^{3+} with the maximum positive charge density and the minimum ion radius among the five investigated metal ions could be coordinated by the secondary N atom on the DTC group. It meant that the functional group with stronger adsorption ability could interact with more species of metal ions. Moreover, the complex structures formed by the four types of functional groups with the same ion became more stable in the order of -NH- on DTC groups, -NH- not on DTC groups, $-NH_2$ not on DTC groups and C=S/C-S on DTC groups, which implied that the removal activity and strength of the four groups were gradually enlarged, and the removal species of metal ions were also increased.

Table 4
Summary for adsorption energies of the five metal ion interacted with different functional groups in cluster of DTCR in Fig. 14.

Figures	Functional groups	Δ *E*(kJ/mol) (-: Structure does not exist)				
		Cr^{3+}	Cu^{2+}	Pb^{2+}	Zn^{2+}	Cd^{2+}
Fig. 14b	C=S/C-S on DTC groups	–323.4	–307.8	–298.5	–294.6	–276.3
Fig. 14d	$–NH_2$ not on DTC groups	–235.9	–217.4	–201.7	–	–
Fig. 14c	–NH- not on DTC groups	–191.2	–168.3	–146.1	–	–
Fig. 14e	–NH- on DTC groups	–102.6	–	–	–	–

Table 4 also revealed that the removal strength of the five metal ions with the same functional group was in the order of $Cr^{3+}>Cu^{2+}>Pb^{2+}>Zn^{2+}>Cd^{2+}$. Considering of the positive charge density and steric hindrance, the metal ion with more positive charge and smaller radius could be more easily adsorbed by the same functional group. The semi diameter of Cr^{3+}, Cu^{2+}, Pb^{2+}, Zn^{2+} and Cd^{2+} was 0.062, 0.072, 0.119, 0.076 and 0.095 nm, respectively, it seemed that the adsorption strength might be in the order of $Cr^{3+}>Cu^{2+}>Zn^{2+}>Cd^{2+}>Pb^{2+}$. However, the hydration ability of the five metal ions should also be taken into account. The hydrated ionic radii of the metals decreased in the order of Pb^{2+} (0.401 nm)>Cu^{2+} (0.419 nm)>Cr^{3+} (0.421 nm)>Cd^{2+} (0.426 nm)> Zn^{2+} (0.430 nm) [38]. The higher hydrated ionic radius of the metal ion meant the greater tendency to be hydrolyzed, which would lead to a reduced sorption [39]. Although the ionic radius of Pb^{2+} was relatively bigger, it had the weakest hydration ability among the five metal ions. So the combined influences of ionic nature and its hydration ability made Pb^{2+} more inclined to be adsorbed than Zn^{2+} and Cd^{2+}. This was in agreement with the study of Hillel, who explained that the smaller the ionic radius and the greater the valence, the more closely and strongly the ion was adsorbed. On the other hand, the greater the ion's hydration, the further it was from the adsorbing surface and the weaker its adsorption [40]. It could be used to explain the calculated result about the removal strength of different irons on the same group as well as the removal species of metal ions on the functional group. Additionally, the difference in the adsorption energies of the metal ions on the same group was small, which stated that there existed competitive adsorption among the adsorbed metal ions.

In the end, the theoretical removal amount of each functional group for the five meal ions is summarized in Table 5 by the modes of metal complexes in Fig. 14 as well as the elemental analysis about the content of functional group in DTCR in Section 3.2.4. It should be noted that there was a hypothesis that there were no tertiary amino groups ($-NR_2$) in the molecule of DTCR, when the maximum removal amount of DTCR for single metal ion was calculated by the theoretical method. Because that the exact contents of $-NR_2$ and other amino groups in unit mass of DTCR could not be obtained by the elemental analysis. By comparison with the experimental removal capacity in Section 3.1.5, the datum in Table 5 demonstrated that the experimental values about Zn^{2+} and Cd^{2+} were very close to the calculated results, since the two kinds of metal ions only interacted with C=S/C-S on DTC groups and 1 mmol metal ions were chelated by 4 mmol of C=S/C-S on DTC groups. While the experimental values about Cr^{3+}, Cu^{2+} and Pb^{2+} were a little lower than the calculated amount. It was possibly caused by the ignored content of tertiary amino groups in the calculation of theoretical values. But the changing trends of the removal amount of the three kinds of metal ions were consistent with that obtained by the theoretical method. This could be used to prove the correctness of the theoretical results about the removal mechanisms.

Table 5
Theoretical capture capabilities of different functional group for the five ions in per mass of DTCR and its comparison with experimental values.

Metal ions	Chelating ability of different functional group for metal ions (mmol:mmol)			Maximum removal amount (mmol/g)	
	-NH- on DTC groups: ions	C=S/C-S on DTC groups: ions	$-NH_2$/-NH- not on DTC groups: ions	Theory	Experiment
Cr^{3+}	1 mol : 1 mol	4 mol: 1 mol	1 mol: 1 mol	2.495	2.16
Cu^{2+}	0	4 mol: 1 mol	1 mol: 1 mol	1.365	1.18
Pb^{2+}	0	4 mol: 1 mol	1 mol: 1 mol	1.365	1.13
Zn^{2+}	0	4 mol: 1 mol	0	0.565	0.58
Cd^{2+}	0	4 mol: 1 mol	0	0.565	0.55

Based on the experimental characterization and theoretical calculation, the relation between the functional groups on DTCR and metal ions could be calculated quantitatively, which would be beneficial to further reveal the removal mechanism and competition mechanism between the adsorbent and different metal ions. It demonstrated that all the five metal ions could be preferentially chelated by C=S/C-S on DTC groups, since the formed metal complexes were the most stable. But there existed an adsorption competition between the five metal ions for this kind of functional group in the solution of mixed metal ions, since the difference in their adsorption energies on this functional group were a little. If there existed a strong competition or there were not enough amounts of DTC groups in the molecule of DTCR, Cr^{3+}, Cu^{2+} and Pb^{2+} could be further adsorbed by other functional groups, such as $-NH_2$ and -NH- which were not on DTC groups. In the same way, Cr^{3+} with the greatest valence and the smallest ionic radius could also be coordinated by the secondary N atom on the DTC group during the process of competitive adsorption or when the other functional groups were inadequate. This could be used to well explain the order of removal ability of DTCR for the five metal ions in the experiments. It also provided a scientific basis for the modification of chelating agents with DTC groups. If the effective content of DTC groups in chelating agent could be raised reasonably, the removal rates of Zn^{2+} and Cd^{2+} in the solution with mixed metal ions would be greatly increased under the same operating conditions.

4. Conclusions

The chelating performance test indicated that DTCR, as a kind of trapping agent for toxic metal ions, could be used to further reduce the concentration of metal ions in the discharged metallic mine water with trace amount of mixed metal ions in Poyang Lake valley. The optimized operating conditions were the volume ratio of DTCR to wastewater with mixed ions about $1:10^4$, pH≈5.5, removal time 20 min and ambient temperature. Under the optimized operating conditions, the removal rate of Cr^{3+}, Cu^{2+}, Pb^{2+}, Zn^{2+} and Cd^{2+} in the treated water could reach 99.70%, 99.28%, 99.10%, 92.33% and 91.49%, respectively, and the residual content of the five ions were 0.003, 0.036, 0.009, 0.383 and 0.085 mg/L, respectively, which were all lower than the contents required in the existing emission standard. The removal ability in the mixed solution followed the order of $Cr^{3+} > Cu^{2+} > Pb^{2+} > Zn^{2+} > Cd^{2+}$.

The experimental characterization revealed that the major functional groups in DTCR were dithiocarbamate groups ($-NCS_2$) and amino groups (-NH-, $-NH_2$ or $-NR_2$) which were not on dithiocarbamate (DTC) groups. The removal mechanisms were investigated by the combination of experimental methods and density functional theory (DFT) calculation, which demonstrated that all the five ions could be captured by C=S/C-S on DTC groups. Moreover, Cr^{3+}, Cu^{2+} and Pb^{2+} could form the coordinate bonds with the N atom of $-NH_2$ and -NH- which were not on the DTC groups. Only Cr^{3+} could be further adsorbed by the secondary N atom on DTC group. The relation between the functional groups and metal ions could be calculated quantitatively based on the removal mechanisms. It could well explain the removal ability order. It could also provide a scientific basis for the further modification and application of chelating agent with DTC groups in the depth treatment of metallic mine wastewater. If the effective content of DTC groups in the chelating agent could be raised reasonably, the removal rates of Zn^{2+} and Cd^{2+} in the solution with mixed metal ions would be greatly increased under the same operating conditions.

Acknowledgements

The authors gratefully acknowledge the financial support provided by National Natural Science Foundation of China (No. 21666021), National Natural Science Foundation of Jiangxi Province (No. 2016BAB203076) and Construction foundation for high level of chemical engineering and technology discipline (No. 100356), Open laboratory Foundation of Poyang lake.

References

[1] Y.H. Wei, J.Y. Zhang, D.W. Zhang, T.H. Tu, L.G. Luo, Metal concentrations in various fish organs of different fish species from Poyang Lake, China, Ecotox. Environ. Safe, 104 (2014) 182–188.

[2] National integrated wastewater discharge standards, China, GB8978–1996.

[3] C.-V. Gherasim, P. Mikulášek, Influence of operating variables on the removal of heavy metal ions from aqueous solutions by nanofiltration. Desalination, 343 (2014) 67–74.

[4] G. Sharma, B. Thakur, Mu. Naushad, A.H. Al-Muhtaseb, A. Kumar, M. Sillanpaa, G.T. Mola, Fabrication and characterization of sodium dodecylsulphate@ ironsilico phosphate nano composite: Ion exchange properties and selectivity for binary metal ions, Mater. Chem. Phys., 193 (2017) 129–139.

[5] G. Sharma, D. Pathania, Mu. Naushad, Preparation, characterization and antimicrobial activity of biopolymer based nano composite ion exchanger pectin zirconium (IV) selenotungsto phosphate: Application for removal of toxic metals, J. Ind. Eng. Chem., 20 (2014) 4482–4490.

[6] H. Guo, Y.Z. Ren, X.L. Sun, Y.D. Xu, X.M. Li, T.C. Zhang, J.X. Kang, D.Q. Liu, Removal of Pb^{2+} from aqueous solutions by a high-efficiency resin, Appl. Surf. Sci., 283 (2013) 660–667.

[7] N. Meunier, P. Drogui, C. Montané, R. Hausler, G. Mercier, J.F. Blais, Comparison between electro coagulation and chemical precipitation for metals removal from acidic soil leachate, J. Hazard. Mater., 137 (2006) 581–590.

[8] G. Sharma, Mu. Naushad, A.H. Al-Muhtaseb, A. Kumar, M.R. Khan, S. Kalia, Shweta, M. Bala, A. Sharma, Fabrication and characterization of chitosan-crosslineked-poly (alginic acid) nanohydrogel for adsorptive removal of Cr(VI) metal ion from aqueous medium, Int. J. Biol. Macromol., 95 (2017) 484–493.

[9] Mu. Naushad, S. Vasudevan, G. Sharma, A. Kumar, Z.A. ALothman, Adsorption kinetics, isotherms, and thermodynamic studies for Hg^{2+} adsorption from aqueous medium using alizarin red-S-loaded amberlite IRA-400 resin, Desal. Water Treat., 57 (2016) 18551–18559.

[10] A. Mittal, Mu. Naushad, G. Sharma, Z.A. ALothman, S.M. Wabaidur, M. Alam, Fabrication of MWCNTs/ThO2 nano composite and its adsorption behavior for the removal of Pb (II) metal from aqueous medium, Desal. Water Treat., 57 (2016) 21863–21869.

[11] G. Sharma, Mu. Naushad, D. Pathania, A. Kumar, A multi functional nano composite pectin thorium(IV) tungstomolybdate for heavy metal separation and photoremediation of malachite green, Desal. Water. Treat., 57 (2016) 19443–19455.

[12] L.H. Liu, Y.H. Li, X. Liu, Z.H. Zhou, Y.L. Ling, Chelating stability of an amphoteric chelating polymer flocculant with Cu (II), Pb (II), Cd (II), and Ni (II), Spectrochim. Acta. A 118 (2014) 765–775.

[13] M. Cegłowski, G. Schroeder, Removal of heavy metal ions with the use of chelating polymers obtained by grafting pyridine-pyrazole ligands onto polymethylhydrosiloxane, Chem. Eng. J., 259 (2015) 885–893.

[14] M. Addy, B. Losey, R. Mohseni, E. Zlotnikov, A. Vasiliev, Adsorption of heavy metal ions on mesoporous silica-modified montmorillonite containing a grafted chelate ligand, Appl. Clay Sci., 59–60 (2012) 115–120.

[15] F.L. Fu, R.M. Chen, Y. Xiong, Application of a novel strategy-Coordination polymerization precipitation to the treatment of Cu^{2+}-containing waste waters, Sep. Purif. Technol., 52 (2) (2006) 388–393.

[16] F.L. Fu, H.Y. Zeng, Q.H. Cai, R.L. Qiu, J. Yu, Y. Xiong, Effective removal of coordinated copper from wastewater using a new dithiocarbamate-type supramolecular heavy metal precipitant, Chemosphere, 69 (2007) 1783–1789.

[17] C.Y. Chen, C.Y. Chen, Stability constants of water-soluble and latex types of chelating polymers containing iminodiacetic acid with some transition-metal ions, Eur. Polym. J., 39 (2003) 991–1000.

[18] X.S. Jing, F.Q. Liu, X. Yang, P.P. Ling, L.J. Li, C. Long, A.M. Li, Adsorption performances and mechanisms of the newly synthesized N,N′-di (carboxymethyl) dithiocarbamate chelating resin toward divalent heavy metal ions from aqueous media, J. Hazard. Mater., 167 (2009) 589–596.

[19] P.F. Yan, M.Y. Ye, S.Y. Sun, X. Xiao, X.J. Lin, W.C. Dai, Research on low-concentration metals removal simultaneously from electroplating wastewater by the method of chelate precipitation-micro filtration, Chinese J. Environ. Eng., 11 (2017) 769–777.

[20] Y.L. Li, L. Liu, Q. Ye, Z.W. Li, Study on the composite sulphuration treatment of metallurgical acidic wastewater containing Cadmium, Ind. Safety Environ. Prot., 43 (2017) 83–87.

[21] P.K. Roy, A.S. Rawat, V. Choudhary, P.K. Rai, Removal of heavy metal ions using polydithiocarbamate resin supported on polystyrene, Ind. J. Chem. Technol., 11 (2004) 51–58.

[22] L. Song, X. Dan, J. Fu, X. Wang, Y. Sheng, X. Liu, DFT investigation of Ni (II) adsorption onto MA-DTPA/PVDF chelating membrane in the presence of coexistent cations and organic acids, J. Hazard. Mater., 199–200 (2012) 433–439.

[23] J. Gao, F. Liu, P. Ling, J. Lei, L. Li, C. Li, A. Li, High efficient removal of Cu (II) by a chelating resin from strong acidic solutions: Complex formation and DFT certification, Chem. Eng. J., 222 (2013) 240–247.

[24] M.J. Frisch, G.W. Trucks, H.B. Schlegel, G.E. Scuseria, M.A. Robb, J.R. Cheeseman, J.A. Jr. Montgomery, T. Vreven, K.N. Kudin, J.C. Burant, J.M. Millam, S.S. Iyengar, J. Tomasi, V. Barone, B. Mennucci, M. Cossi, G. Scalmani, N. Rega, G.A. Petersson, H. Nakatsuji, M. Hada, M. Ehara, K. Toyota, R. Fukuda, J. Hasegawa, M. Ishida, T. Nakajima, Y. Honda, O. Kitao, H. Nakai, M. Klene, X. Li, J.E.Knox, H.P. Hratchian, J.B.Cross, C. Adamo, J. Jaramillo, R. Gomperts, R.E. Stratmann, O. Yazyev, A.J. Austin, R. Cammi, C. Pomelli, J.W. Ochterski, P.Y. Ayala, K. Morokuma, G.A. Voth, P. Salvador, J.J. Dannenberg, V.G. Zakrzewski, S. Dapprich, A.D. Daniels, M.C. Strain, O. Farkas, D.K. Malick, A.D. Rabuck, K. Raghavachari, J.B. Foresman, J.V. Ortiz, Q. Cui, A.G. Baboul, S. Clifford, J. Cioslowski, B.B. Stefanov, G. Liu, A. Liashenko, P. Piskorz, I. Komaromi, R.L. Martin, D.J. Fox, T. Keith, M.A. Al-Laham, C.Y. Peng, A. Nanayakkara, M. Challacombe, P.M.W. Gill, B. Johnson, W. Chen, M.W. Wong, C. Gonzalez, J.A. Pople, Gaussian03, Revision C.01; Gaussian Inc.: Wallingford, CT, 2004.

[25] X.X. Wang, Z.S. Chen, S.B. Yang, Application of graphene oxides for the removal of Pb (II) ions from aqueous solutions: Experimental and DFT calculation, J. Mol. Liq., 211 (2015) 957–964.

[26] X.D. Gao, G. Yang, R. Tian, W.Q. Ding, F.N. Hu, X.M. Liu, H. Li, Formation of sandwich structure through ion adsorption at the mineral and humic interfaces: A combined experimental computational study, J. Mol. Struct., 1093 (2015) 96–100.

[27] S.F. Sousa, P.A. Fernandes, M.J. Ramos, General performance of density functionals, J. Phys. Chem., A 111 (2007) 10439–10452.

[28] L. Bai, H. Hu, W. Fu, J. Wan, X. Cheng, L. Zhuge, L. Xiong, Q. Chen, Synthesis of a novel silica-supported dithiocarbamate adsorbent and its properties for the removal of heavy metal ions, J. Hazard. Mater., 195 (2011) 261–275.

[29] S.H. Dar, S. Thirumaran, S. Selvanayagam, Synthesis, spectral and X-ray structual studies on Hg(II) dithiocarbamate complexes: A new precursor for HgS nano particles, Polyhedron 96 (2015) 16–24.

[30] H.B. Zhen, Q. Xu, Y.Y. Hu, J.H. Chen, Characteristics of heavy metals capturing agent dithiocarbamate (DTC) fro treatment of ethylene diamine tetraacetic acid-Cu (EDTA-Cu) contaminated wastewater, Chem. Eng. J., 209 (2012) 547–557.

[31] R. Payne, R.J. Magee, J. Liesegang, Infrared and X-ray photo electron spectroscopy of some transition metal dithiocarbamates and xanthates, J. Electron. Spectrosc. Relat. Phenom., 35 (1985) 113–130.

[32] M. Saad, C. Gaiani, M. Mullet, J. Scher, B. Cuq, X-ray Photo electron Spectroscopy for wheat powders: measurement of surface chemical composition, J. Agric. Food Chem., 59 (2011) 1527–1540.

[33] C. Ji, S. Song, C. Wang, C.M. Sun, R.J. Qu, C.H. Wang, H. Chen, Preparation and adsorption properties of chelating resins containing 3-aminopyridine and hydrophilic spacer arm for Hg(II), Chem. Eng. J., 165 (2010) 573–580.

[34] Q. Li, J. Yu, F. Zhou, X. Jiang, Synthesis and characterization of dithiocarbamate carbon nanotubes for the removal of heavy metal ions from aqueous solutions, Colloid. Surface, A 482 (2015) 306–314.

[35] F.H. Wang, W.Y. Shi, Z.L. Wang, Quantum chemistry study on six heavy metal ions complexes with dimethyldithiocarbamate, Comput. Appl. Chem., 29 (2012) 647–650.

[36] A.P. Balasubramaniam, P. Anssi, L. Manu, M. Manickavachagam, K. Erkki, H. Esa, S. Mika, Synthesis and structural studies on Ni(II) dithiocarbamates: Exploring intra,molecular Ni · ·H–C interactions, Polyhedron 123 (2017) 453–461.

[37] Y. Niu, S. Feng, Y. Ding, R. Qu, D. Wang, J. Han, Theoretical investigation on sulfur-containing chelating resin-divalent metal complexes, Int. J. Quantum. Chem., 110 (2010) 1982–1993.

[38] M. Mahmood-ul-Hassan, V. Suthor, E. Rafique, M. Yasin, Removal of Cd, Cr and Pb from aqueous solution by unmodified and modified agricultural wastes, Environ. Monit. Assess, 187 (2015) 19–26.

[39] C.K. Danny, K. Chun, W. Cheung, K.H. Keith, F. John, G. McKay, Sorption equilibria of metal ions on bone char, Chemosphere, 54 (2004) 273–281.

[40] D. Hillel, Environmental soil physics, San Diego, Academic Press 1998.